JTTEE5 9:121-127

Long-Term Cyclic Oxidation Behavior of Uncoated and Coated RE108 and IN939 at 980 and 870 °C

K.N. Lee, C.A. Barrett, and J. Smith

(Submitted 30 December 1999; in revised form 5 December 1999)

Very long-term cyclic oxidation behavior of Re108 and In939 with and without a protective coating was evaluated at 980 and 870 °C, respectively. Re108 and In939 without a protective coating began to show a rapid weight loss at 3000 h due to scale spallation, indicating the need for an oxidation protective coating for longer than thousands of hours of oxidative life. NiAl-base coatings of a vapor phase aluminide (VPA), a pack aluminide (CODEP), and a slurry paint aluminide (SERMALOY J) were applied on Re108 and In939. The VPA and CODEP on Re108 and all three coatings on In939 showed excellent cyclic oxidation resistance out to 10,000 h. Coated alloys were annealed in an inert atmosphere to determine the loss of Al from the coating into the alloy substrate through diffusion. The Al loss from the coating through diffusion was twice as great as the Al loss through oxidation after 10,000 h of cyclic exposure. The oxidation life of VPA-coated Re108 was estimated by calculating the amount of Al initially available for protective oxidation and the amount of Al lost through oxidation and diffusion.

Keywords cyclic oxidation, oxidative life, Re108, In939, VPA, SERMALOY J

1. Introduction

Oxidation protection of high-temperature alloys relies on the formation of an external layer of stable, slow growing oxides, such as Cr_2O_3, Al_2O_3, or SiO_2, through the selective oxidation of Cr, Al, or Si, respectively.[1] There is a critical value for each of these elements, which is necessary to form a continuous external oxide layer of respective element in isothermal oxidation.[1] Therefore, the protection conferred by Al_2O_3, for example, ends once the selective oxidation of Al reduces the Al content in the alloy below the critical value. Consequently, the oxidative lifetime of an alumina-forming alloy at a given temperature can be estimated by calculating the amount of Al initially available for protective oxidation and the loss of Al through oxidation, assuming rapid diffusional kinetics in the alloy. [2,3]

Enhanced efficiency and performance of gas turbine engines requires hot section structural components with higher temperature capability and longer life. In a typical alumina-forming high-temperature superalloy, there is only a limited amount of excess Al above the critical value because too much of Al degrades the mechanical strength of superalloys. Under thermal cycling, protective scales crack and spall due to the difference in thermal expansion between the alloy and the scale, accelerating the loss of Al compared with that in isothermal exposure. Thus, an external coating with a large reservoir of Al above the critical content is needed for a long cyclic oxidative life at elevated temperatures. In coated alloys, diffusion between the coating and the substrate is another source for the loss of the element responsible for the protective oxidation.[4]

In this study, the long-term cyclic oxidation kinetics of alumina-forming Re108 and chromia-forming In939 with and without an external coating (NiAl-base coatings) were investigated. Coated alloys were also exposed in an inert atmosphere to investigate the chemical interdiffusion between the coating and the superalloy substrate. Oxidation life of coated Re108 was estimated on the basis of oxidation kinetics and diffusion data.

2. Experimental Procedure

Oxidation coupons of Re108 and In939 ($2.5 \times 1.25 \times 0.3$ cm), both supplied by GE Aircraft Engines, Cincinnati, OH, were cut from a large plate of each respective alloy. The as-cast Re108 has a surface layer (~25 μm thick) depleted in Cr, W, and Co.[5] The surfaces of a second set of coupons was ground off to remove the depleted surface layer. Some as-cast coupons were coated with a vapor phase aluminide (VPA, supplied by GE Aircraft Engines, Cincinnati, OH), a pack aluminide (CODEP, supplied by GE Aircraft Engines), and a slurry paint aluminide (SERMALOY J,

K.N. Lee, Cleveland State University, Cleveland, OH 44135, Resident Scientist at NASA Glenn Research Center, Cleveland, OH 44135; and **C.A. Barrett,** NASA Glenn Research Center, Cleveland, OH 44135. **J. Smith,** Dynacs, Cleveland, OH 44135.

Table 1 Nominal composition of Re108 and In939 (wt.%)

Alloy	Ni	Al	Cr	Co	W	Ta	Ti	Hf	Mo	Fe	Si
Re108	Bal	5.7	8.5	9.9	8.5	2.88	0.79	1.09	0.55	0.04	0.03
In939	Bal	2	22	19	2	1.5	3.6	...	...	...	...

supplied by Pratt & Whitney, West Palm Beach, FL.). The VPA and CODEP were about 40 μm thick and SERMALOY J was about 60 μm thick. All three coatings are based on NiAl. Tables 1 and 2, respectively, show the nominal composition of Rel08 and In939 and the composition of the three coatings as determined in this study using electron microprobe analysis (EMPA). For the coating, the average composition of each element across the coating measured at 5 μm intervals is reported (Table 2). Uncoated coupons were polished to a 600-grit surface finish and all coupons were rinsed in acetone and methyl alcohol in an ultrasonic cleaner prior to the cyclic oxidation or chemical diffusion test.

A cyclic oxidation test was performed using an automated cyclic furnace.[6] Each cycle consisted of 1 h at temperature and a minimum of 20 min at room temperature. Typically, samples reached the test temperature within 2 min and the ambient temperature within 5 min in each cycle. Oxidized coupons were weighed periodically using a microbalance (±0.02 mg) to determine the oxidation kinetics. Chemical diffusion was carried out in a horizontal furnace in a flowing Ar-5%H_2 to minimize the oxidation of coupons. Both cyclic oxidation and chemical diffusion tests were performed at 980 and 870 °C, respectively, for Re108 and In939.

X-ray diffraction was used to determine the phases present in the oxide scale and the coating, and scanning electron microscopy (SEM) equipped with energy dispersive spectroscopy was used to examine the cross sections of post-oxidation and post-diffusion coupons. Electron microprobe analysis was used to determine the compositional profile of various elements along the cross section of postdiffusion coupons.

3. Results And Discussion

3.1 Oxidation of Uncoated Re108 and In939

Figure 1 shows the oxidation kinetics of as-cast and ground Re108 after cyclic oxidation at 980 °C. Both coupons showed an initial parabolic oxidation followed by a constant weight period and eventually a weight loss after 3000 h. Except for the slightly higher weight loss rate after 3000 h in the ground coupon, the two coupons showed a similar oxidation behavior. Fig. 2 shows the cross section of Re108 after 4500 h. The oxide scale consists of a NiO top layer, an intermediate spinel layer, and an inner Al_2O_3 layer. There are also islands of HfO_2 particles mostly within the spinel layer. X-ray diffraction on the Re108 coupon after 4500 h showed NiO, HfO_2, spinel, Al_2O_3, and TiO_2.

Figure 3 shows the oxidation kinetics of In939 after cyclic oxidation at 870 °C. The weight change behavior was very similar to that of Re108 at 980 °C, with the ground In939 showing a slightly higher weight loss rate. Fig. 4 shows the cross section of In9393 after 4500 h. The oxide scale consists of a NiO top layer, an intermediate spinel layer, and an inner Cr_2O_3 layer, similar to Re108 except that the inner Al_2O_3 was replaced by Cr_2O_3. X-ray diffraction showed NiO, spinel, Cr_2O_3, and TiO_2.

The kinetics data shown in Fig. 1 and 3 are typical of alumina- or chromia-forming superalloys under cyclic oxidation, *i.e.*, initial weight gain followed by a weight loss due to scale spallation (paralinear oxidation). The rapid weight loss rate of Re108 and In939 indicates the need for protective coatings for an oxidation life beyond thousands of hours.

Table 2 Composition of VPA, CODEP, and SERMALOY J coatings determined in this study by EMPA (wt.%)

Coating	Ni	Al	Cr	Co	Si
VPA	Bal	31.29	1.79	6.41	. . .
CODEP	Bal	35.45	1.47	5.67	. . .
SERMALOY J	Bal	27.43	15.74	13.54	7.04

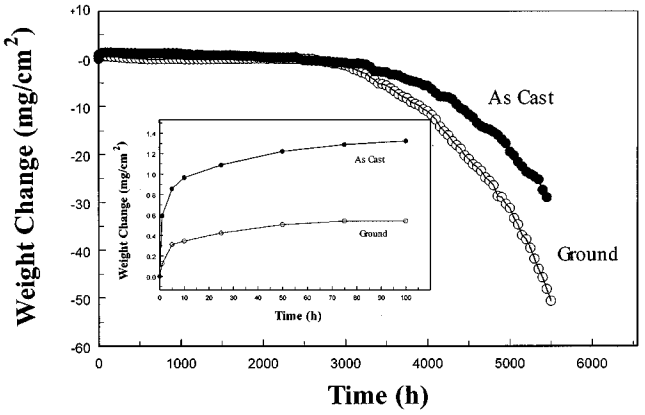

Fig. 1 Oxidation kinetics of Re108 at 980 °C with 1 h cycle.

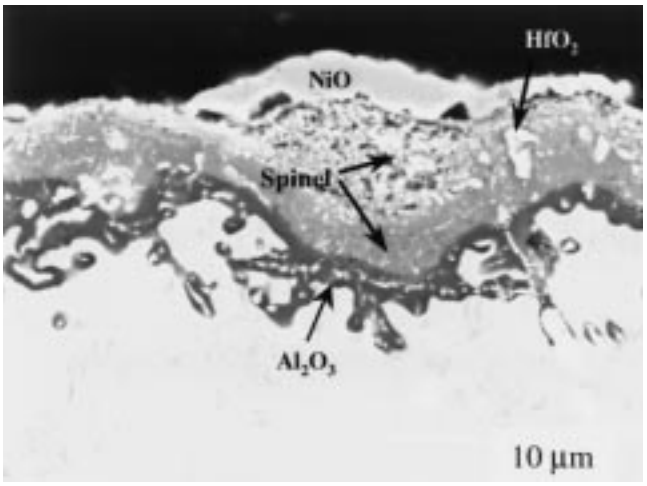

Fig. 2 Cross section of Re108 after 4500 h at 980 °C with 1 h cycle.

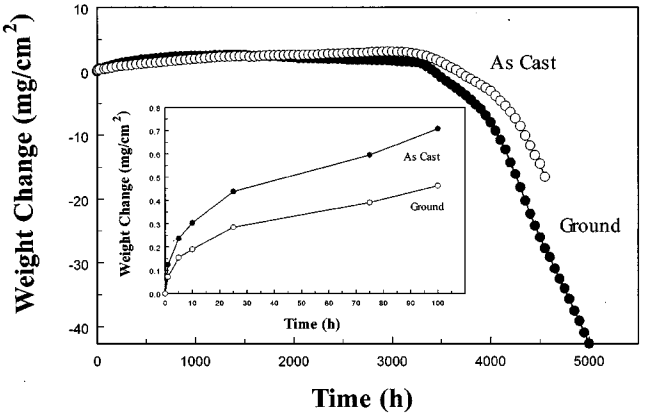

Fig. 3 Oxidation kinetics of In939 at 870 °C with 1 h cycle.

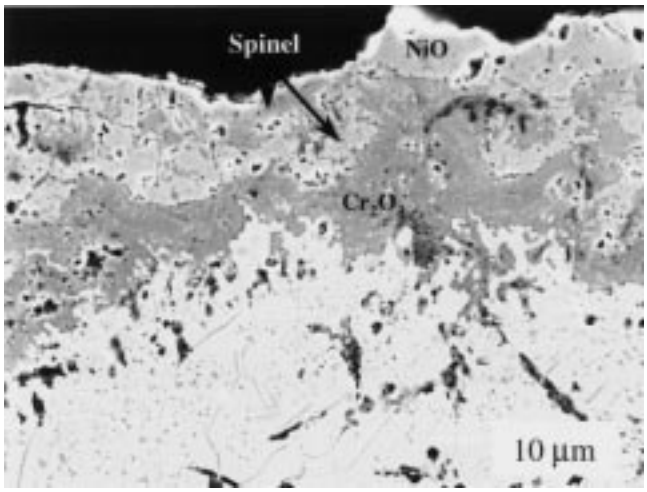

Fig. 4 Cross section of In939 after 4500 h at 870 °C with 1 h cycle.

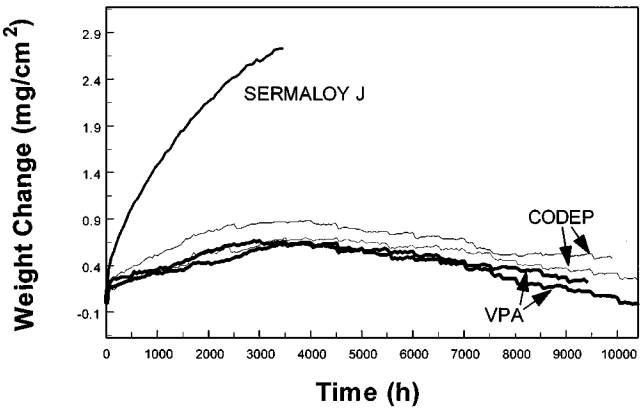

Fig. 5 Oxidation kinetics of coated Re108 at 980 °C with 1 h cycle.

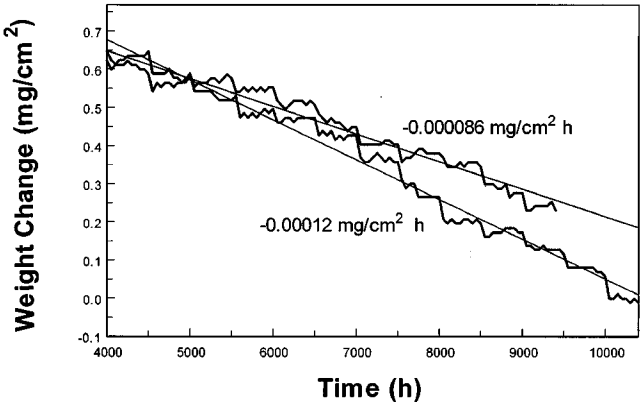

Fig. 6 Linear weight loss rate of VPA-coated Re108 at 980 °C with 1 h cycle.

3.2. Oxidation of Coated Re108 and In939

NiAl-base coatings of VPA, CODEP, and SERMALOY J were applied on Re108 and In939 for extended oxidation protection. The coating composition determined by EMPA in this study is shown in Table 2.

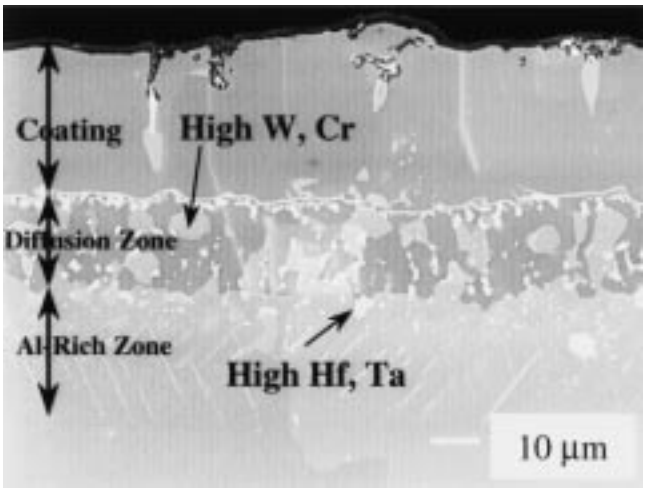

(a)

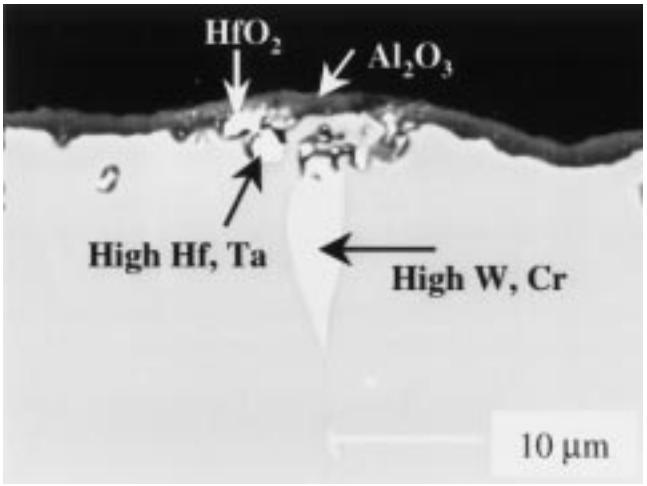

(b)

Fig. 7 Cross section of VPA-coated Re108 after 1000 h at 980 °C with 1 h cycle: (**a**) low magnification showing the coating and the diffusion zone and (**b**) high magnification showing the oxide scale.

Re108. Figure 5 shows the oxidation kinetics of coated Re108 after cyclic oxidation at 980 °C. The two sets of data for CODEP and VPA are replicates. The CODEP and VPA showed a typical paralinear weight change of alumina-forming alloys under cyclic oxidation. No significant scale spallation was observed during the weight gain period, indicating that the weight change in this period was predominantly due to the formation of alumina scale. SERMALOY J gained substantially higher weight than VPA or CODEP when the test was terminated at 3500 h. A significant amount of spinel was observed in the scale of SERMALOY J coating, which presumably was responsible for the higher weight gain of this coating. The transition from weight gain to weight loss occurred at around 4000 h for VPA and CODEP. The weight loss was fairly linear out to 10,000 h (Fig. 6).

Figure 7 shows the cross section of VPA-coated Re108 after 1000 h. The scale was mostly Al_2O_3 with some isolated patches of HfO_2. The brightest phase in the coating was rich in Hf and Ta, from which HfO_2 fore4med. The bright phase in the coating was rich in W and Cr (Fig. 7b). The diffusion zone contained

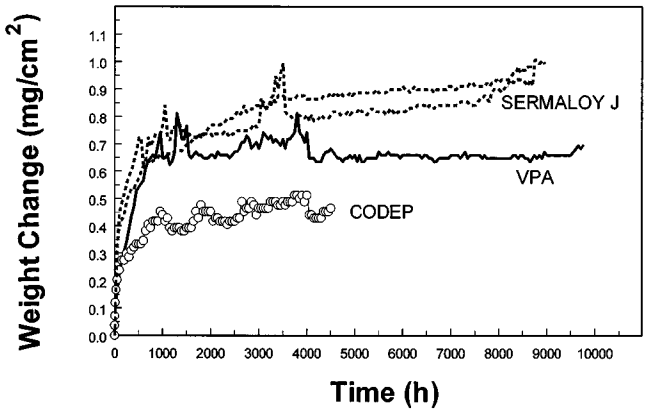

Fig. 8 Oxidation kinetics of coated In939 at 870 °C with 1 h cycle.

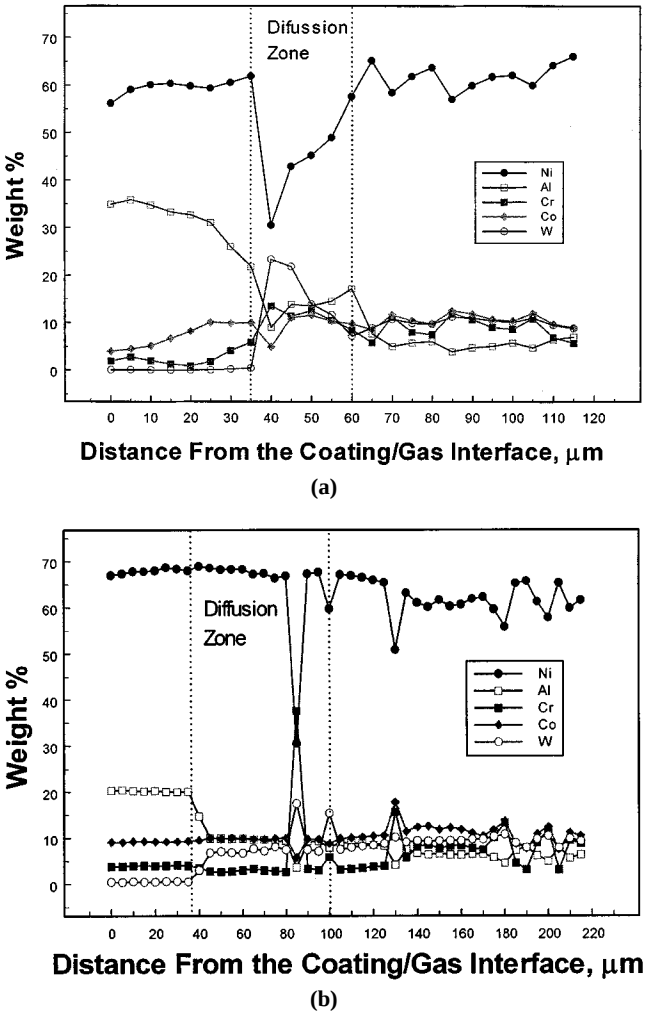

Fig. 9 Concentration profile of elements in VPA-coated Re108: (**a**) as-processed and (**b**) 9000 h in Ar-5%H_2.

significant amounts of Hf/Ta- and W/Cr-rich phases. Below the diffusion zone was a zone rich in aluminum, which contained a needle-shaped second phase rich in W and Cr (Fig. 7a).

IN939. Figure 8 shows the oxidation kinetics of coated In939 after cyclic oxidation at 870 °C. All three coatings showed an initial rapid weight gain (transient oxidation) followed by a very slow, steady-state weight gain. The SERMALOY J and VPA showed higher initial weight gains than CODEP; however, the steady-state oxidation rate was similar in all three coatings. Note that the weight gain of SERMALOY J-coated In939 at 870 °C was significantly lower than that of SERMALOY J-coated Re108 at 980 °C (Fig. 5). The oxide scale of SERMALOY J coating contained a smaller amount of spinel at the lower temperature.

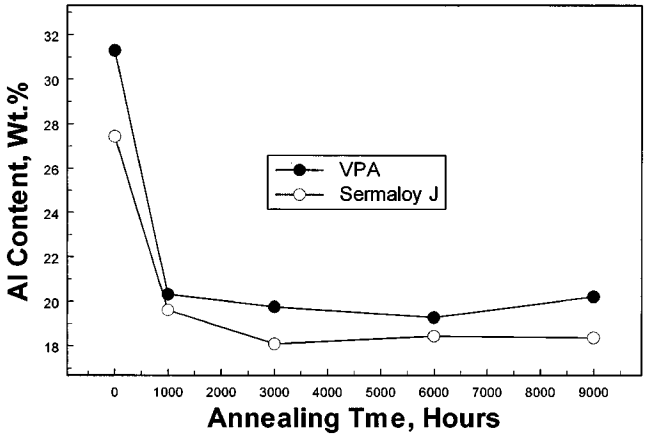

Fig. 10 Plot of Al concentration in the coating versus the annealing time (VPA: 980 °C, SERMALOY J: 870 °C).

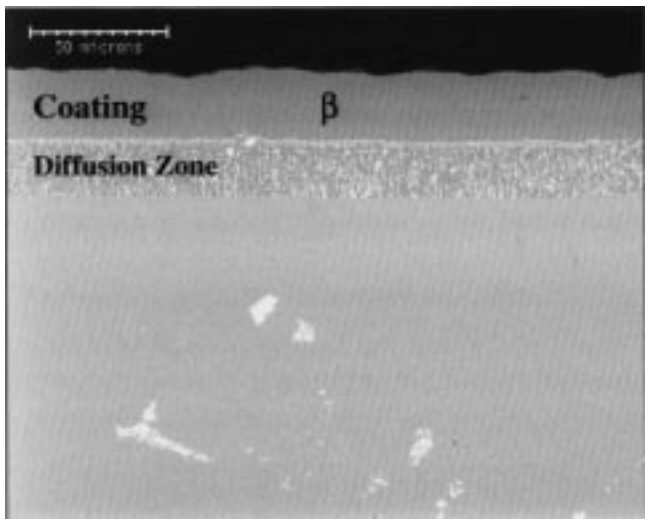

Fig. 11 Cross section of as-processed VPA-coated Re108

3.3. Chemical Diffusion

VPA-Coated Re108. Figures 9a and b show the concentration profiles of various elements along the coating/diffusion zone/ substrate after 0 and 9000 h annealing, respectively, at 980 °C. Two points are worth mentioning. After the heat treatment, concentration profiles of all elements became fairly flat and the diffusion zone extended significantly. The flattening of elemental concentration profiles occurred within the first 1000 h annealing. Fig. 10 shows the plot of Al concentration in the coating versus annealing time for VPA-coated Re108. Note the rapid drop of Al concentration within the first 1000 h after which it leveled off at 20 to

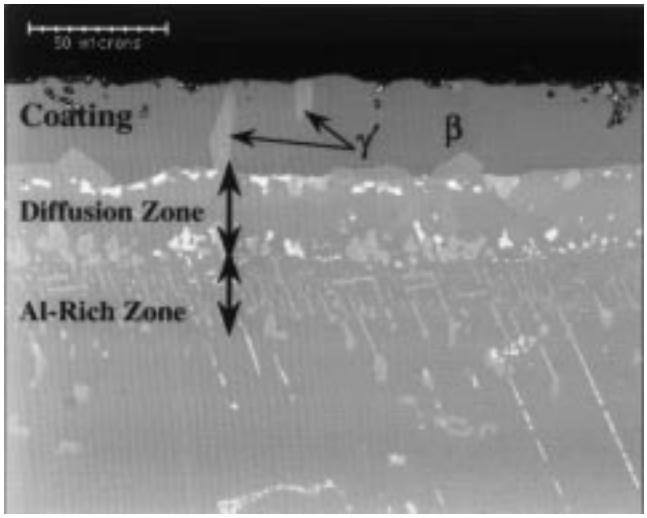

(a)

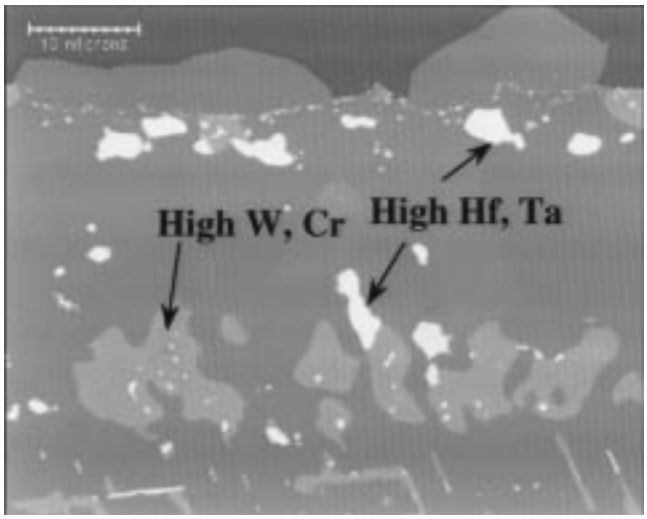

(b)

Fig. 12 Cross section of VPA-coated Re108 after 9000 h in Ar-5%H_2 at 980 °C: (**a**) low magnification showing the coating and the diffusion zone and (**b**) high magnification showing the diffusion zone.

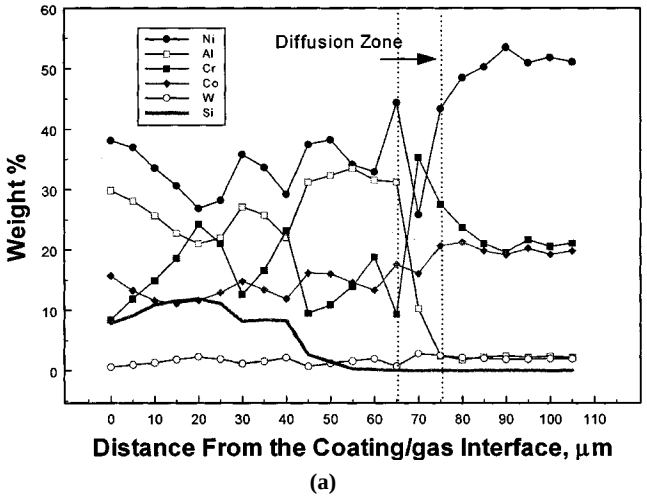

(a)

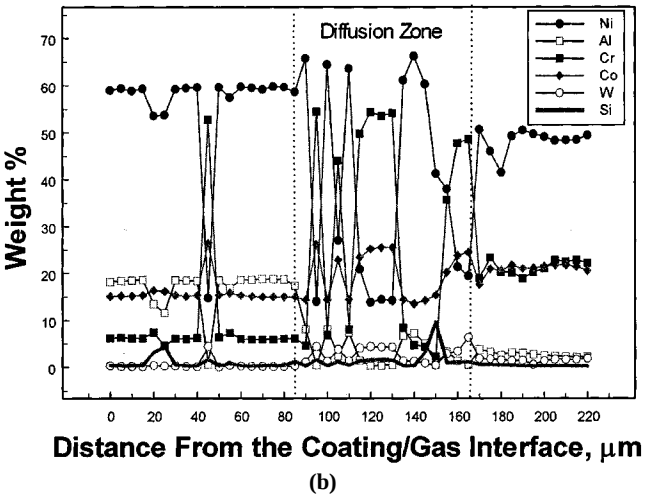

(b)

Fig. 13 Concentration profile of elements in SERMALOY J-coated In939: (**a**) as-processed and (**b**) 9000 h in Ar-5%H_2.

21 wt.%, indicating the initial rapid diffusion of Al out of the coating. Fig. 11 and 12 compare the cross sections of as-processed and annealed (9000 h) VPA-coated Re108. The as-processed VPA coating was β phase (Fig. 11), while the γ' second phase appeared after annealing (Fig. 12a). The diffusion zone contained two second phases, *i.e.*, Hf/Ta-rich phase (brightest) and W/Cr-rich phase (bright). Note that the second phases significantly coarsened with annealing (Fig. 12b). An Al-rich zone, containing a high concentration of a needle-shaped phase, developed below the diffusion zone (Fig. 12a). This second phase was rich in W and Cr.

SERMALOY J-Coated In939. Fig. 13a and b show the concentration profiles of various elements along the coating/diffusion zone/substrate after 0 and 9000 h annealing, respectively, at 870 °C. Similar behavior to the VPA coating was observed, *i.e.*, the concentration profiles of all elements became fairly flat after annealing and the diffusion zone thickness increased significantly. Fig. 14 and 15 compare the cross sections of as-processed and annealed (9000 h) SERMALOY J-coated In939. A high concentration of a second phase rich in Cr, Co, and W precipitated in the coating after the annealing (Fig. 15). The diffusion zone, after annealing, consisted of at least three phases (Fig. 15), the detailed analysis of which was not attempted in this study. Similar to VPA, the second phase below the diffusion zone was needle shaped (Fig. 15). Fig. 10 shows the plot of Al concentration in the coating versus annealing time for SERMALOY J-coated In939. Similar to VPA, rapid diffusion of Al occurred within the first 1000 h, after which it leveled off at 18 to 19 wt.%.

3.4. Oxidation Life Projection of VPA-Coated Re108

Oxidation life of an alumina-forming alloy ends when the Al concentration in the alloy drops below the critical Al concentration, which is necessary for the formation of a continuous, protective Al_2O_3 scale.[1] In other words, oxidation life ends when all the Al available (excess Al above the critical value) is lost. There are two sources for the loss of Al, *i.e.*, oxidation to form Al_2O_3 scale and diffusion between the coating and the substrate.

Since the scale formed on VPA was mostly Al_2O_3, the loss of Al through oxidation was determined from the oxidation weight change. The Al loss during the weight gain period was determined from the stoichiometry of the reaction of Al with O_2 to form Al_2O_3 scale, assuming that scale spallation was negligible during this period. The Al loss rate during the weight loss period was taken from the average slope of the weight loss curve and was assumed to be applicable to the end of oxidation life. The projected oxidative lifetime of bulk NiAl using this assumption agreed fairly well with the lifetime determined by experiments.[2] The change in Al concentration with annealing (Fig. 10) was used to determine the loss of Al through diffusion.

Calculation of Al Available. Consider a unit volume ($1 \times 1 \times h$ cm; h = coating thickness) of VPA coating. The fraction of Al initially available for protective oxidation is related to the initial fraction of Al and the critical Al concentration according to Eq 1.

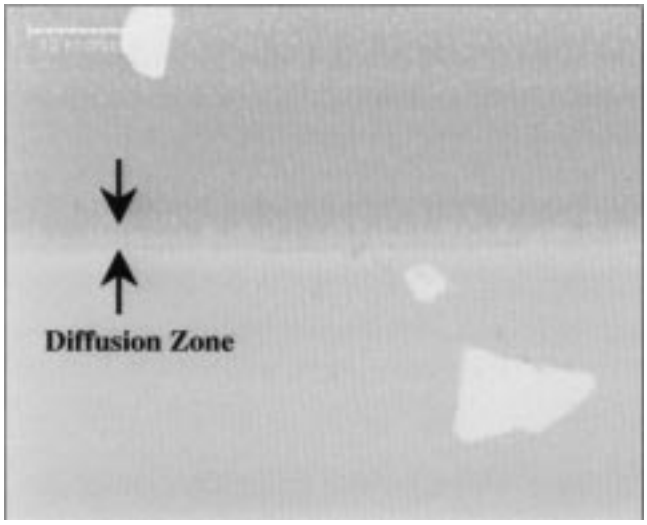

Fig. 14 Cross section of as-processed SERMALOY J-coated In939.

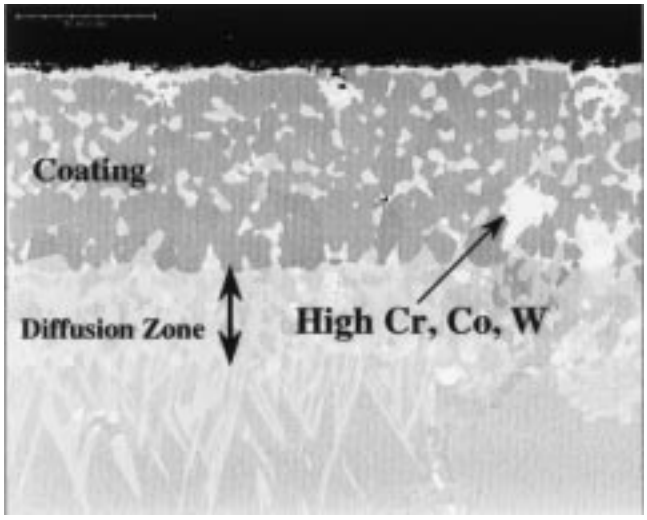

Fig. 15 Cross section of SERMALOY J-coated In939 after 9000 h in Ar-5%H_2 at 870 °C.

$$f_{\mathrm{Al,avail}} = f_{\mathrm{Al}}{}^{o} - f_{\mathrm{Al}}{}^{*} \quad \text{(Eq 1)}$$

where

$f_{\mathrm{Al,\,avail}}$ is the weight fraction of Al initially available for protective oxidation,

$f_{\mathrm{Al}}{}^{o}$ is the initial weight fraction of Al, and

$f_{\mathrm{Al}}{}^{*}$ is the weight fraction of Al at the time of oxidative failure.

Thus, the weight of Al initially available for protective oxidation in the unit area of coating is given by

$$W_{\mathrm{Al,avail}} = \left(f_{\mathrm{Al}}{}^{o} - f_{\mathrm{Al}}{}^{*}\right) \rho \cdot h \ \mathrm{mg/cm^2} \quad \text{(Eq 2)}$$

where

ρ is the coating density (mg/cm^3) and

h is the coating thickness (cm)

Calculation of Al Lost. *Al Loss during the Weight Gain Period:* The Al loss during the weight gain period is calculated from the parabolic oxidation equation, assuming that the scale spallation was negligible during this period. The parabolic rate constant was determined from the slope of (weight gain)^2 versus time plot. The loss of Al through spallation needs to be taken into consideration for more rigorous calculation of Al loss during the weight gain period of a cyclic oxidation.[7]

$$(W_p)^2 = k_p \cdot t \quad \text{(Eq 3)}$$

where

W_p is the weight gain by parabolic oxidation,

k_p is the parabolic rate constant, and

t is the oxidation time.

Rearranging Eq 3 and taking the stoichiometry of alumina formation reaction into consideration, the loss of Al during the weight gain period is given by

$$W_{\mathrm{Al},p} = 1.125(k_p t)^{0.5} \ \mathrm{mg/cm^2} \ (t < t^*) \quad \text{(Eq 4)}$$

where

t^* is the time at the transition from weight gain to linear weight loss period.

Al Loss during the Linear Weight Loss Period: During the weight loss period, the rate of Al loss is taken from the average slope of the weight loss curve and is assumed to be applicable to the end of oxidation life. Thus, the loss of Al during this period is given by

$$W_{\mathrm{Al},l} = k_l(t - t^*)\, mg/cm^2 \ (t > t^*) \quad \text{(Eq 5)}$$

where

k_l is the average weight loss rate (mg/cm^2 h).

Loss of Al through Diffusion: Two key assumptions in this calculation are that the loss of Al through diffusion is negligible at $t > 1000$ h (based on the data in Fig. 10) and the coating density is constant throughout the coating life. Although the coating density undoubtedly will change to some degree as the coating composition changes, this assumption may be justifiable considering the approximate nature of the life projection in this study. Thus,

the weight fraction of Al in the coating after diffusion anneal in an inert atmosphere is given by

$$f_{Al}^{**} = f_{Al}^{o} - f_{Al,d} \quad \text{(Eq 6)}$$

where

f_{Al}^{**} is the weight fraction of Al in the coating after diffusion anneal in inert atmosphere and

$f_{Al,d}$ is the weight fraction of Al lost by diffusion.

Rearranging Eq 6, the weight fraction of Al lost by diffusion is given by

$$f_{Al,d} = f_{Al}^{o} - f_{Al}^{**} \quad \text{(Eq 7)}$$

Thus, the weight of Al lost by diffusion from the unit are of coating is given by

$$W_{Al,d} = \left(f_{Al}^{o} - f_{Al}^{**}\right)\rho \cdot h \text{ mg/cm}^2 \ (t > 1000\text{h}) \quad \text{(Eq 8)}$$

Oxidation Life Projection. Oxidation life ends when the available Al, $W_{Al,\,avail}$ (Eq 2), equals the Al lost, *i.e.*, $W_{Al,\,p}$ (Eq 4) + $W_{Al,\,l}$ (Eq 5) + $W_{Al,\,d}$ (Eq 8). In other words, the oxidation life ends when the following condition is met:

$$\left(f_{Al}^{o} - f_{Al^*}\right)\rho \cdot h = 1.125\left(k_p t\right)^{0.5} + k_l\left(t - t^*\right) + \left(f_{Al}^{o} - f_{Al}^{**}\right)\rho \cdot h \quad \text{(Eq 9)}$$

All parameters in Eq 9 are known except for f_{Al}*. Table 3 lists the values of the parameters in Eq 9. Nesbitt *et al.* reported that the critical Al concentration in the cyclic oxidation of NiAl at 1200 to 1400 °C was ≅20 wt.%.[2] As will be shown in the following discussion, the critical Al concentration in the cyclic oxidation of VPA coating in this study was less than 14 wt.%, indicating the dependence of the critical Al concentration on alloy composition. Using Eq 9, the oxidation life, t_{life}, can be plotted as a function of the critical Al concentration, f_{Al}* (Fig. 16). If the critical Al concentration were 14 wt.%, the coating would fail at t = 10,000 h. This indicates that the aluminum concentration in the coating at t = 10,000 h was 14 wt.%, which is a drop of ~18 wt.% from the initial concentration (~32 wt.%). (Fig. 16 can be interpreted as a plot of oxidation time versus Al concentration in the coating.) Since about 11.5 wt.% was lost through diffusion (Fig. 10), the remainder (~6.5 wt.%) was lost through oxidation, which was about half of what was lost through diffusion. This demonstrates the importance of Al loss through diffusion in the consideration of the oxidation lifetime of coated alloys. The critical Al concentration of the VPA coating used in this study needs to be determined to project the cyclic oxidation life using Eq 9. One way is to perform an accelerated oxidation at higher temperature until the coated coupon fails and then analyze the Al content in the coating using EMPA.

4. Conclusions

- Re108 and In939 need a protective coating for a cyclic oxidation life longer than thousands of hours at T > 980 and 870 °C, respectively.

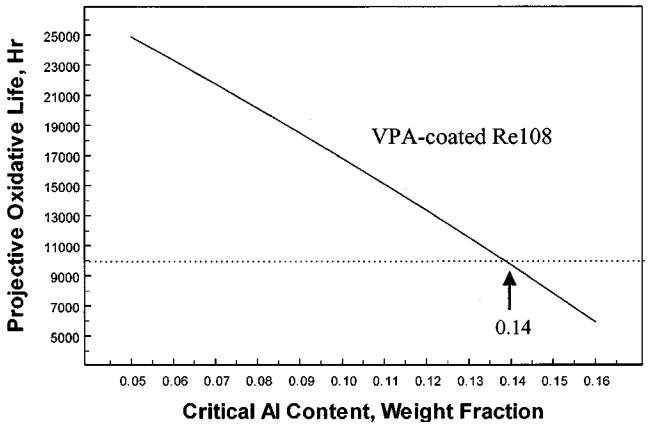

Fig. 16 Plot of oxidative life vs critical Al content for VPA-coated Re108 at 980 °C with 1 h cycle.

Table 3 The values of the parameters in Eq 9

f_{Al}^{o}	f_{Al}**	ρ(mg/cm^3)	h(μm)	t* (h)	k_p (mg^2/cm^{4}h)	k_l (mg/cm^{2}h)
0.32	0.20	6000	40	4000	0.00011	0.00012

- The VPA and CODEP coatings on Re108 and VPA, CODEP, and SERMALOY coatings on In939 showed excellent oxidation resistance out to 10,000 h at 980 and 870 °C, respectively.
- A substantial amount of Al was lost from the coating into the substrate through diffusion. In the case of VPA-coated Re108, the Al loss through diffusion was twice as great as the Al loss through oxidation after 10,000 h cyclic exposure at 980 °C.
- The critical Al concentration of VPA coating needs to be determined to project the oxidation life of VPA-coated Re108.

Acknowledgments

We are grateful to B.K. Gupta of GEAE for the supply VPA- and CODEP-coated Re198 coupons and M. Maloney of Pratt & Whitney for the supply of SERMALOY J-coated In939 coupons. We are also grateful to J.W. Sweeney of Dynacs, NASA Glenn Group, for the SEM of postdiffusion coupons.

References

1. N. Birks and G.H. Meier: *Introduction to High Temperature Oxidation of Metals*, Edward Arnold, London, 1983, ch. 5.
2. J.A. Nesbitt, E.J. Vinarcik, C.A. Barrett, and J. Doychak: *Mater. Sci. Eng.*, 1992, vol. A153, pp. 561-66.
3. K.N. Lee, V. Arya, C.A. Barrett, and G. Halford: *Metall. Mater. Trans. A*, 1996, vol. 27A, pp. 3279-91.
4. J.L. Smialek and C.E. Lowell: *J. Electrochem. Soc.*, 1974, vol. 121 (6), pp. 800-05.
5. Jon Schaeffer: GE Aircraft Engines, Cincinnati, OH, unpublished research, 1994.
6. C.A. Barrett and C.E. Lowell: *J. Test. Eval.*, 1982, vol. 10 (6), pp. 273-78.
7. C.E. Lowell, C.A. Barrett, R.W. Palmer, J.V. Auping, and H.B. Probst: *Oxid. Met.*, 1991, vol. 36 (1-2), pp. 81-112.